 ©2011 Kvantovaya Elektronika and Turpion Ltd

PACS numbers: 42.62.Be; 42.30.Ms; 87.64.M–
DOI: 10.1070/QE2011v041n04ABEH014603

Speckle-correlation analysis of the microcapillary blood circulation in nail bed

M.A. Vilensky, D.N. Agafonov, D.A. Zimnyakov, V.V. Tuchin, R.A. Zdrazhevskii

Abstract. **We present the results of the experimental studies of the possibility of monitoring the blood microcirculation in human finger nail bed with application of speckle-correlation analysis, based on estimating the contrast of time-averaged dynamic speckles. The hemodynamics at normal blood circulation and under conditions of partially suppressed blood circulation is analysed. A microscopic analysis is performed to visualise the structural changes in capillaries that are caused by suppressing blood circulation. The problems and prospects of speckle-correlation monitoring of the nail bed microhemodynamics under laboratory and clinical conditions are discussed.**

Keywords: *speckles, speckle-correlation monitoring, microcirculation, capillaroscopy, nail bed.*

1. Introduction

Cardio-vascular complications, atherosclerosis, diabetes mellitus, chronic venous insufficiency, and some other diseases are accompanied by functional and morphological changes in the microcirculation bed. In modern medicine the problems related to the mechanisms of microcirculation are of key importance for studying the system of blood circulation as a whole. Indeed, the processes occurring between microvessels and tissues in various organs serve to deliver oxygen and other necessary substances to individual organs and remove their functioning products. The study of the microcirculation system became fruitful due to the harmonic combination of conventional and new morphological and functional analytical methods. The methods used by morphologists for studying the microcirculation bed on autopsic and biopsic materials have a number of drawbacks: first, the state of intramural vessels is mainly determined on transverse and skew cuts and, second, there are significant difficulties in studying simultaneously hemo-circulation and lymph-circulation vessels. The morphological microcirculation studies, which were performed in most cases by the biopsy method, reflect the microcirculation state only at some specific point and cannot reflect dynamic processes.

The development of laser Doppler fluometry [1, 2], capillaroscopy [3, 4], intravital microscopy [5], optical coherent tomography [6], magneto-resonance tomography [7], radioisotope arteriography, etc. has made it possible to perform one's life-time dynamic study of the microcirculation state. Some of these methods have a number of limitations: spatial and time resolution, insufficient information about the particle flux, incomplete information obtained by scanning over depth because of possible invasiveness of measurements, etc. Currently, the most effective diagnostic methods for determining the main parameters of microcirculation are the methods of dynamic light scattering (DLS): laser Doppler fluometry (LDF), speckle visualisation, and methods of computer biomicroscopy.

The physical basis of DLS methods is the Doppler modulation of the scattered radiation frequency upon interaction of coherent light field with moving scatterers. When coherent light is scattered by an ensemble of moving particles, the scattered light field is a superposition of partial frequency-modulated fields, scattered from individual particles in the volume probed. The generally accepted approach to study the dynamics of scatterers in a probed volume is the spectral or correlation analysis of the fluctuations of scattered light intensity at a fixed observation point.

The LDF method is used, for example, to estimate the state of blood microcirculation for patients with various diseases of the cardio-vascular system and damage of the microcirculation system in diabetology, cardiology, gastroenterology, dermatology, and stomatology. The LDF-based LAKK-01 instrument is successfully applied in clinical practice [8]. The main drawback of this approach is that it fails to determine the motion rate of blood cells in capillaries in physical units.

One of the high-resolution microscopic approaches that are widely used to monitor the microcirculation state is video capillaroscopy; it is successfully applied in clinical studies and dermatology [3, 4]. This method makes it possible to perform online visualisation (for example, for capillaries in the skin dermis), which is clinically important for such some pathologies as skin damage, decubital ulcer, or diabetes [9, 10]. Generally, video capillaroscopy is used in clinical diagnostics for certain skin areas (nail bed, pigmented regions), where capillaries are located close to the surface. To reduce the effect of multiple scattering and increase efficiency, various antireflection agents are often applied [11–14]. The purpose of this method is to estimate various morphological and functional parameters of

M.A. Vilensky, D.N. Agafonov N.G. Chernyshevsky National Research Saratov State University, ul. Astrakhanskaya 83, 410012 Saratov, Russia; e-mail: vilenskyma@mail.ru;
D.A. Zimnyakov, R.A. Zdrazhevskii Saratov State Technical University, ul. Politekhnicheskaya 77, 410054 Saratov, Russia; Institute of Precise Mechanics and Control, Russian Academy of Sciences, ul. Rabochaya 24, Saratov, 410028 Russia; e-mail: zimnykov@mail.ru, sweetnuts@inbox.ru;
V.V. Tuchin N.G. Chernyshevsky National Research Saratov State University, ul. Astrakhanskaya 83, 410012 Saratov, Russia; Institute of Problems of Precise Mechanics and Control, Russian Academy of Sciences, ul. Rabochaya 24, 410028 Saratov, Russia; e-mail: tuchinvv@mail.ru

Received 17 March 2011
Kvantovaya Elektronika **41** (4) 324–328 (2011)
Translated by Yu.P. Sin'kov

capillary bed, for example, to measure the capillary diameter and the capillary network density and sinuosity. However, this approach is rather difficult to apply to certain types of pigmented skin, where melanin very strongly absorbs light in the visible spectral range. Fluorescent markers are used in these situations, due to which the method becomes invasive to a certain extent. Another drawback of video capillaroscopy is that it yields no information over depth.

There is an interesting modification of this method, which was referred to as the polarisation-sensitive capillaroscopy (PSC). For example, a polarisation-sensitive capillaroscope was used in [15, 16] to reveal pathologies in the microcirculation bed at sickle cell anemia. This disease is caused by the mutation of β-hemoglobin gene, which leads to the formation of anomalous hemoglobin HbS. A change in the properties of polymerised hemoglobin chain at this mutation leads to a change in the properties of the entire molecule and the formation of a 'sticky' area on the hemoglobin surface. When hemoglobin is deoxygenated, this area 'opens' and bounds one hemoglobin molecule S with other similar molecules. The result is the polymerisation of hemoglobin molecules and formation of large protein rods, which cause deformation and hemolysis of erythrocytes passing through capillaries. These changes were monitored by measuring the polarisation state during hemoglobin polymerisation for isolated erythrocytes, as well as the changes in the blood circulation rate caused by the sickle shape of cells, which impedes their free passage through capillaries.

Combination of DLS methods and microscopy yields a high-efficiency tool for determining the microcirculation parameters. Such attempts have been made since the beginning of the 1970s [15, 17]. Speckle microscopy was used to estimate the changes in the contrast of speckle patterns for individual capillaries. For example, a speckle microscope with an ultrahigh spatial resolution was used in [18] to reveal the effect of preparation toxicity on the microcirculation state. As a result not only the duration of the toxic action of photoinactivated vaccines but also the nature of their effect was estimated.

Here, we used the speckle-contrast method (one of the laser speckle visualisation methods) to monitor the hemodynamics of blood in nail bed capillaries. This simple and high-efficiency method (which is used, in particular, to visualise blood circulation) was proposed in the middle of the 1990s and referred to as LASCA (LAser Speckle Contrast Analysis) [19]. It is based on the proximity of statistical moments of spatial and temporal intensity fluctuations of ergodic and statistically uniform speckle-fields, which are estimated by averaging over time and space [20–22]. This technique suggests estimation of the contrast of time-averaged dynamic speckles as a function of time-averaged speckle-modulated images: $V(T) = \delta I(T)/\langle I \rangle$, where $\langle I \rangle$ and $\delta I(T)$ are, respectively, the mean-square and rms values of brightness fluctuations of a speckle-modulated image at a specified averaging time T.

To implement online measurements, it is necessary to average speckle images over a time interval from 5 to 30 ms. The rate of contrast decay for speckles recorded with an increase in the averaging time depends on the mean time of displacement of mobile scatterers in the volume probed by a distance equal to the probe light wavelength in the medium and on the average number of scattering events during light propagation through the volume probed. An analysis of the local estimates of the contrast of speckle-modulated images of the object surface at a fixed exposure time over zones covering a specified number of speckles makes it possible to visualise areas where the characteristics of scatter mobility differs significantly from the values averaged over the region probed. The maximum sensitivity of this method to variations in the mobility of dynamic scatterers over the region probed is obtained by choosing an exposure time corresponding to the maximum (in magnitude) value of the derivative $\mathrm{d}V(T)/\mathrm{d}T$. Full-field speckle correlometry, which is based on the analysis of the contrast of time-averaged speckle-modulated images, was successfully applied under laboratory and clinical conditions to study blood microcirculation in burn-damaged skin [23] and in the cerebral cortex of laboratory animals after taking medicines [24], to investigate the kinetics of thermal modification of cartilaginous tissues under IR laser radiation [25–27], etc. [28].

Possible LASCA applications include, for example, examination of the state of diabetes mellitus patient by monitoring the blood microcirculation in the patient nail bed. Diabetes mellitus is a chronic polyetiologic disease; it is characterised by significant violations of the carbohydrate, fat, protein, and mineral exchange, which result in violation of microcirculation. For example, children with labile diabetes mellitus have a characteristic blush (diabetic rubeosis), which is caused by expansion of skin capillaries [29]. The most significant changes in diabetes patients occur at the microcirculation bed level. They are characterised by a decrease in the linear blood circulation rate, aggregation and stagnation of blood corpuscles, and an increase in the vessel permittivity. Microcirculation violations have a generalised character, occur in several stages, and depend generally on the form of diabetes and the degree of the tissue damage caused by diabetes. Monitoring of microhemodynamics in nail bed capillaries would make it possible to reveal regularities of pathological process caused by diabetes and control the treatment.

2. Experimental

Speckle-correlation monitoring of microhemodynamics variations in nail bed was performed on a laboratory sample of full-field speckle-correlation capillaroscope (Fig. 1). The radiation source was a single-mode helium–neon GN-5P laser. An LOMO microlens (20×, NA = 0.40) was used to expand the laser beam. Speckle-modulated images of the area analysed were recorded by a Basler A602f monochromatic CMOS camera (656×491 pixels in the matrix, pixel size 9.9×9.9 μm, 8 bit pixel^{-1}), equipped with an LOMO objective with a focal

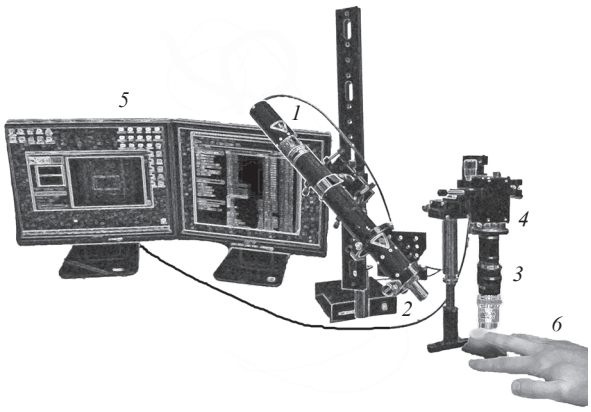

Figure 1. Experimental setup:
(*1*) helium–neon GN-5P laser, (*2*) beam expander, (*3*) camera objective, (*4*) Basler A602f CMOS camera, (*5*) computer, and (*6*) object.

distance $f = 30$ mm. The camera was controlled during alignment and subsequent detection of video data using a specialised program written in the LabView environment; the video data were recorded on a hard disk for subsequent analysis in the AVI format without compression, which provided a constant frame-to-frame interval in subsequent partition of the video data into sequences of dynamic speckle images. Data were detected with a frame frequency of 40 Hz in the subframe regime with a window size of 1×5 pixels and frame exposure time of 20 ms. The camera parameters (magnification, brightness), depending on the optical characteristics of biological tissue, were automatically chosen so as to ensure the maximum spread of pixel brightnesses over the area analysed in the absence of saturation of individual image elements (the maximum pixel brightness within the area analysed did not exceed 200 units). Figure 2 shows as an example the full-frame images of recorded speckle structures for a human nail bed under the conditions of short-term hemodynamics suppression and at normal blood circulation.

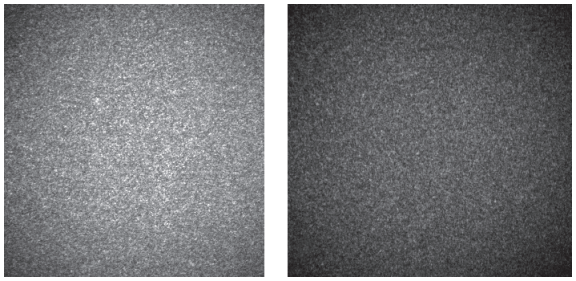

a b

Figure 2. Full-frame images of recorded speckle-structures (a) under the conditions of short-term suppression of hemodynamics and (b) at normal blood circulation.

During the treatment of speckle-modulated images of an area of internal-organ surface we calculated the contrast $V_k = \sigma_{Ik}/\bar{I}_k$, where k is the frame number in the sequence of speckle-modulated images, $\bar{I}_k$ is the frame-averaged brightness, and σ_{Ik} is the rms value of the fluctuation component of pixel brightness:

$$\bar{I}_k = \frac{1}{MN}\sum_{m=1}^{M}\sum_{n=1}^{N} I_k(m,n);$$

$$\sigma_{Ik} = \left[\frac{1}{MN}\sum_{m=1}^{M}\sum_{n=1}^{N}\{I_k(m,n) - \bar{I}_k\}^2\right]^{1/2}.$$

Here, M and N are, respectively, the numbers of pixels in the rows and columns of the fragment analysed and $I_k(m,n)$ is the m,nth pixel brightness in the kth frame. If V_k is used as a diagnostic parameter, the variations in the contrast of speckle-modulated images averaged over the exposure time are analysed; for statistically homogeneous ergodic dynamic speckle-structures the contrast of time-averaged speckles is related to the normalised time correlation function of intensity fluctuations $g_2(\tau)$ as follows [22, 30]:

$$V(T) = \left[\frac{1}{T}\int_0^T g_2(\tau)\mathrm{d}\tau\right]^{1/2}, \qquad (1)$$

where τ is the exposure time;

$$g_2(\tau) = \langle[I(t+\tau) - \langle I\rangle][I(t) - \langle I\rangle]\rangle/\langle[I(t) - \langle I\rangle]^2\rangle.$$

As was shown in some studies (see, for example, [15, 24]), when detecting backscattered laser radiation from the surface layers of biological tissues with pronounced microhemodynamics, the time correlation function of the scattered light intensity fluctuations allows (with acceptable accuracy) an exponential approximation in the form $g_2(\tau) \approx \exp(-\tau/\tau_c)$, where the correlation time of intensity fluctuations, τ_c, is determined by the characteristic time of displacement of dynamic scatterers (erythrocytes) by a distance of about the probe light wavelength λ and by the optical characteristics of the medium probed: $\tau_c \approx K\lambda/\bar{v}$ (here, K is the coefficient depending on the detection geometry and the optical characteristics of the biological tissue in the region analysed and $\bar{v}$ is the average velocity of erythrocyte motion through microcapillaries).

Using the full-field speckle correlometry based on the analysis of the contrast of time-averaged speckle-modulated images, one can establish the following relationship between the variations in contrast and the average velocity of erythrocytes in the volume probed [20]:

$$\delta V(T) = -\left\{\frac{1}{2V(T)}\frac{1}{T}\int_0^T \frac{\partial[g_2(\tau)]}{\partial\bar{v}}\mathrm{d}\tau\right\}\delta\bar{v}. \qquad (2)$$

Within the model of dynamic scattering of probe laser radiation with an exponentially decaying autocorrelation function of intensity fluctuations $g_2(\tau) = \exp(-\tau\bar{v}/K\lambda)$, this expression can be transformed as follows: $\delta V(T) = \{C(T)/[2K\lambda V(T)]\}\delta\bar{v}$; the parameter $C(T) = (1/T)\int_0^T \tau g_2(\tau)\mathrm{d}\tau$ can be interpreted as the estimated (with respect to the finite data sample time T) ratio of the first moment of the correlation function $g_2(\tau)$ to the sample time. For the accepted dynamic scattering model one can show that $C(T) \to 0$ at $T \ll \tau_c$ and $T \gg \tau_c$ and reaches a maximum at $T \sim \tau_c$. This circumstance determines the optimal conditions for detecting speckle-modulated images, at which the full-field speckle-correlation method has maximum sensitivity.

The experiment was performed with five volunteers, which did not suffer diseases related to the cardio-vascular system. The fourth finger of the left hand of each volunteer was investigated at normal blood circulation in the hand and under partial blockade. Blood circulation was blocked by cross-clamping the main arteries with an elastic cuff of a Medica CS-105 tonometer. The degree of cross-clamping (monitored by a built-in manometer) was kept the same in all cases. The experiments were performed at constant room temperature (23–25 °C).

The blood circulation blockade decreases microcirculation. Immediately after the blockade reactive postocclusive hyperemia develops; under normal conditions it manifests itself in an increase in blood circulation to a level exceeding the initial one. To monitor the morphological changes in capillaries under partial blockade of blood circulation, we performed microscopic studies based on visualisation of capillaries using a computer capillaroscope, equipped with a Basler A602f monochromatic CMOS camera and an LOMO microlens ($8^{\times}$, NA = 0.20). The diameter of the illuminated area was fixed (0.5 mm), and the video camera exposure time was 25 ms.

To reduce the effect of light scattering in cellular structures and biological tissues in microscopic measurements, we used optical blooming, which implies coating a tissue by an

immersion material – antireflection agent with a high osmolarity and a refractive index, exceeding that of the intratissue fluid. The composition of this material was 95% glycerol : dimethyl sulfoxide (DMSO) : water = 1 : 1 : 1. The microcirculation state was monitored 4 min after depositing the antireflection agent.

Figure 3 shows images of a nail bed area with capillaries before and after depositing an antireflection agent. The photographs were made with an interval of 4 min. This value was chosen based on the data of other researchers*.

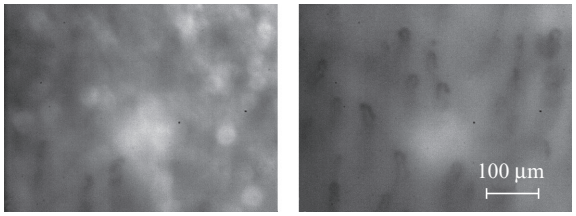

Figure 3. Images of a nail bed area with capillaries (a) before and (b) after depositing an antireflection agent.

The thickness of the epidermis horny layer in the area of volunteer nail bed under study was 0.19±0.12 mm. DMSO was used to enhance transdermal transport of acting agents (glycerol solution), because, being a bipolar aprotic solvent, it is an efficient conductor of various molecules through the skin horny layer.

3. Speckle-correlation analysis of the capillary blood circulation in nail bed

According to the microscopy data, the diameter of visible capillary before and after the blood circulation blockade was, respectively, 7.5 and 11 μm, which indicated a partial decrease in the microcirculation level in the tissue. Similar conclusions can be drawn based on Fig.4, which presents the time dependence of the contrast of averaged dynamic speckle-fields (the averaging was over five independent measurements of microcirculation contrast for five volunteers).

The contrast data were obtained for three steady-state physiological regimes. During the first 10 s of the blood circulation blockade (the first physiological regime) the contrast corresponded to a level of 0.6; then postocclusive hyperemia was observed during the next ten seconds (the second physiological regime), with a decrease in contrast to 0.38; and, finally, the microcirculation restored to the initial level with a slight increase in contrast to 0.42 (the third physiological regime). Note that the use of antireflection agent did not affect the ratio of the obtained values of the speckle-image contrast before and after the blood circulation blockade but excluded the effect of multiple scattering (increase in contrast at zero scatterer velocities). In addition, the application of an antireflection agent made it possible to perform microscopic measurements with a higher accuracy and sensitivity.

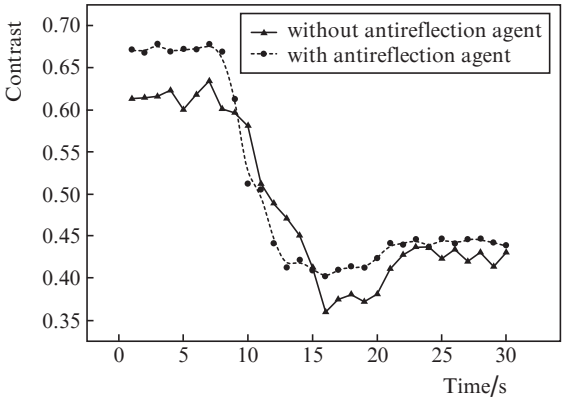

Figure 4. Time dependence of the contrast of averaged dynamic speckle-fields.

4. Conclusions

We demonstrated the efficiency of monitoring the microhemodynamics of nail bed capillaries by full-field speckle correlometry in order to determine the potential of this method under laboratory and clinical conditions. The contrast of time-averaged dynamic speckles, which is used as a diagnostic parameter, is characterised by a fairly high sensitivity to changes in the blood microcirculation under external factors. One of possible promising applications of this method in clinical practice is the monitoring of microhemodynamics at diabetes and other diseases that affect microcirculation for diagnostics and monitoring therapy performed.

Acknowledgements. This study was supported by the Russian Foundation for Basic Research (Grant Nos 09-02-01048-a and 224014); Grant PHOTONICS4LIFE-FP7-ICT-2007-2; projects of the Ministry of Education and Science of the Russian Federation (Nos 1.4.09, 2.1.1/4989 and 2.2.1.1/2950); and State Contracts of the Russian Federation (Nos 02.740.11.0484, 02.740.11.0770, and 02.740.11.0879).

References

1. Leahy M.J., de Mul F.F., Nilsson G.E., Maniewski R. *Technol. Health Care*, **7**, 143 (1999).
2. Yaoeda K., Shirakashi M., Funaki S., Nakatsue T., Abe H. *Am. J. Ophtalmol.*, **129**, 734 (2000).
3. Hanazawa S., Prewitt R.L., Terzis J.K. *J. Reconstr. Microsurg.*, **10**, 21 (1994).
4. Dixon J.B., Zawieja D.C., Gashev A.A., Coté G.L. *J. Biomed. Opt.*, **10**, 064016 (2005).
5. Lipowsky H.H., Sheikh N.U., Katz D.M. *J. Clin. Invest.*, **80**, 117 (1987).
6. Chen Z.P., Milner T.E., Dave D., Nelson J.S. *Opt. Lett.*, **22**, 64, (1997).
7. Schvartzman P.R., White R.D. *Textbook of Cardiovascular Medicine*. Ed. by E.J. Topol (Philadelphia: Lippincott Williams & Wilkins, 2002).
8. Gurfinkel' Yu.I., Makeeva O.V., Ostrozhinskii V.A. *Funkt. diagnost.*, **2**, 18 (2010).
9. Ryan T.J., in *The Physiology and Pathophysiology of the Skin*. Ed. by A. Jarrett (London: Academic Press, 1973) Vol. 1, p. 653.

* The *in vivo* diffuse reflectance spectra of rat skin, recorded at different instants after hypodermic injection of glycerol solution, were analysed in [16, 31]. During the first 3.5–4 min the diffuse reflectance of hind skin area (with an average skin thickness of 0.57±0.16 mm) decreased on average by 16%, without a change in the spectral shape. During the next 5–6 min the diffuse reflectance increased by approximately 20%, also without a change in the spectral shape, after which the signal level did not change up to the end of the measurements.

10. Fagrell B., Fronek A., Intaglietta M.A. *Am. J. Physiol.*, **233**, 318 (1977).
11. Galanzha E.I., Tuchin V.V., Solovieva A.V., Stepanova T.V., Luo Q., Cheng H. *J. Phys. D: Appl. Phys.*, **36**, 1739 (2003).
12. Bashkatov A.N., Korolevich A.N., Tuchin V.V., Sinichkin Y.P., Genina E.A., Stolnitz. M.M., Dubina N.S., Vecherinski S.I., Belsley M.S. *Asian J. Phys.*, **15** (1), 1 (2006).
13. Dolezalova P., Young S.P., Bacon P.A., Southwood T.R. *Ann. Rheum. Dis.*, **62**, 444 (2003).
14. Ohtsuka T., Tamura T., Yamakage A., Yamazaki S. *Br. J. Dermatol.*, **139**, 622 (1998).
15. Riva C.E., Ross B., Benedek G.B. *Invest. Ophthalmol.*, **11**, 936 (1972).
16. Morgan S.P., Stockford I.M. *Advanced Optical Cytometry: Methods and Disease Diagnoses* (Weinheim: Wiley, 2011) p. 433–462.
17. Mishina H., Asakura T., Nagai S. *Opt. Commun.*, **11**, 99 (1974).
18. Ulyanov S.S. *Physiol. Meas.*, **22**, 681 (2001).
19. Tuchin V.V. *Lazery i volokonnaya optika v biomeditsinskikh issledovaniyakh* (Lasers and Fiber Optics in Biomedical Studies) (Moscow: Fizmatlit, 2010) p. 155.
20. Briers J.D., Webster S. *J. Biomed. Opt.*, **1**, 174 (1996).
21. Briers J.D., Richards G.J., He X.W. *J. Biomed. Opt.*, **4** (1), 164 (1999).
22. Tuchin V.V. *Opticheskaya biomeditsinskaya diagnostika* (Optical Biomedical Diagnostics) (Moscow: Fizmatlit, 2007) p. 284.
23. Briers J.D. *Physiol. Meas.*, **22**, 35 (2001).
24. Dunn A.K. *J. Cerebr. Blood Flow Metab.*, **21**, 195 (2001).
25. Zimnyakov D.A. *Appl. Opt.*, **41** (28), 5984 (2002).
26. Zimnyakov D.A. *Appl. Opt.*, **45** (18), 4480 (2006).
27. Zimnyakov D.A. *Zh. Fiz. Khim.*, **81** (4), 725 (2007).
28. Timerbulatov V.M. (Ed.) *Primenenie lazernoi doplerovskoi floumetrii v endoskopii i endokhirurgii pri neotlozhnykh zabolevaniyakh organov bryushnoi polosti* (Application of Laser Doppler Fluorimetry in Endoscopy and Endosurgery at Acute Diseases of Abdominal Cavity Organs) (Moscow: MEDpress-inform, 2006) p. 17.
29. Efimov A.S. *Klinicheskaya diabetologiya* (Clinical Diabetology) (Kiev: Zdorov'e, 1998) p. 85.
30. Le T.M., Paul J.S., Al-Nashash H., Tan A., Luft A.R., Sheu F.S., Ong S.H. *IEEE Trans. Med. Imaging*, **26** (6), 833 (2007).
31. Genina E.A., Bashkatov A.N., Sinichkin Yu.P., Tuchin V.V. *Opt. Spektrosk.*, **109** (2), 256 (2010).